POLITECNICO DI TORINO
Repository ISTITUZIONALE

Evaluation of porosity and degree of saturation from seismic and electrical data

Original
Evaluation of porosity and degree of saturation from seismic and electrical data / Cosentini, R.M., Foti, S.. - In: GEOTECHNIQUE. - ISSN 0016-8505. - STAMPA. - 64:4(2014), pp. 278-286. [10.1680/geot.13.P.075]

Availability:
This version is available at: 11583/2544350 since:

Publisher:
Thomas Telford

Published
DOI:10.1680/geot.13.P.075

Terms of use:

This article is made available under terms and conditions as specified in the corresponding bibliographic description in the repository

Publisher copyright

(Article begins on next page)

15 November 2026

Cosentini, R. M. & Foti, S. (2014). *Géotechnique* **64**, No. 4, 278–286 [http://dx.doi.org/10.1680/geot.13.P.075]

Evaluation of porosity and degree of saturation from seismic and electrical data

R. M. COSENTINI* and S. FOTI*

The characterisation of unsaturated intermediate and coarse-grained soils faces some practical difficulties because undisturbed sampling is not easy. Geophysical methods provide useful information as they can be applied on site for testing geo-materials in their natural state. Moreover their repeated application over time is effective and efficient for monitoring purposes. A procedure for evaluating porosity and degree of saturation on the basis of electrical resistivity and wave velocities measurements is proposed. The approach is based on an electro-seismic model that utilises Archie's law to describe the electrical behaviour of soils and a recent formulation of elastic wave propagation in unsaturated soils. The proposed procedure is applied to laboratory data, and shows promising results.

KEYWORDS: geophysics; laboratory tests; partial saturation; suction; waves and wave loading

INTRODUCTION

The evaluation of physical properties of soils is easily performed with standard methods if undisturbed samples are available. For fine-grained soils, porosity, water content and other physical parameters are currently measured in the laboratory. For coarse-grained soils, it is complicated to obtain undisturbed samples unless sophisticated and expensive techniques, such as ground freezing (Hofman *et al.*, 2000), are used. Moreover, ground freezing requires full saturation, hence it is not suited to unsaturated soils. Therefore, there is a need for alternative procedures based on in-situ testing.

In geotechnical engineering, empirical correlations with penetration tests are widely used to estimate the relative density of coarse-grained soils. These correlations are calibrated for specific soils (e.g. clean quartz sands). Furthermore, the experimental data, from which the correlations are derived, are typically widely dispersed, hence the confidence limits are very large (see e.g. Lancellotta, 2009). These aspects limit the application of empirical relationships to certain types of soils and the accuracy of the obtained values is poor. The in-situ water content is typically measured by indirect methods (capacitance/frequency-domain reflectometry probes (FDR), time-domain reflectometry probes (TDR), dual needle heat pulse probes, tensiometers). For these techniques, relationships between measured physical soil parameters and soil water content need to be specifically calibrated. Moreover some disadvantages are observed: they allow only point measurements; some types of equipment have a narrow operational range; they require accurate installation because they are very sensitive to air gaps at the contact with the soil.

Geophysical testing provides valuable approaches based on the measurements of geophysical parameters from which physical parameters of soils can be inferred. These techniques allow large volumes of soil to be investigated and preserve the initial structure of soil deposits. Moreover, geophysical tests may be performed from the ground surface, providing non-invasive investigation methods. Also, they require only transportable equipment, allowing tests to be performed in difficult logistical conditions of terrain (e.g. steep slopes). Geophysical parameters, such as the electrical resistivity (ρ) and seismic wave velocities (V_P, V_S), depend on physical and mechanical properties of soils. The relationships between geophysical parameters and physical properties are not unique, as they depend on the choice of the constitutive model. For example, Foti *et al.* (2002) used the theory of linear poro-elasticity (Biot, 1956a, 1956b) for determining porosity in fluid-saturated soil deposits from values of V_S and V_P measured with cross-hole seismic tests. The accuracy of the approach has been investigated by Foti & Lancellotta (2004) considering a total of over 250 determinations of soil porosity. The average difference between soil porosity from seismic velocities and measured porosity on laboratory samples was found to be consistently below 10%.

In unsaturated soils, the multiphase system includes a solid skeleton and pores filled by more than one fluid (e.g. air and water). Seismic velocities are then not sufficient to fully characterise the porous medium. A possible strategy requires additional information that may be obtained for example from geo-electrical measurements. Soil porosity and degree of saturation may be evaluated through an appropriate electro-seismic model – that is, a relationship between geophysical parameters and physical properties.

The combination of different geophysical datasets, such as geo-electric and geo-seismic measurements, generates synergies for improving the interpretation and the reliability of their results. For example, joint inversion processes can be formulated to share common unknowns of the different geophysical models (e.g. layer geometry), thus getting a better constrained inverse problem (Comina *et al.*, 2002; Foti *et al.*, 2003). A stronger level of integration between different geophysical datasets can be obtained with physical coupling of model parameters, as in the approach proposed in the present paper.

The non-destructive approach for the evaluation of soil density and water content proposed by Fratta *et al.* (2005) is an example of combination of geophysical measurements. Their method involves measuring the dielectric permittivity and P-wave velocity of soils as the water content is increased.

This paper proposes a strategy to evaluate the porosity and the degree of saturation of unsaturated soils using

Manuscript received 17 May 2013; revised manuscript accepted 13 February 2014. Published online ahead of print 19 March 2014. Discussion on this paper closes on 1 September 2014, for further details see p. ii.

* Department of Structural Building and Geotechnical Engineering (DISEG), Politecnico di Torino, Torino, Italy.

seismic and electrical resistivity measurements. The proposed electro-seismic model is based on a simplified formulation of wave propagation in unsaturated soils proposed by Conte *et al.* (2009) and on the Archie's law (Archie, 1942) that links electrical resistivity of soil with porosity, degree of saturation and electrical resistivity of the fluid. The model is applied to laboratory data to check its applicability.

DESCRIPTION OF THE PROPOSED MODEL

Theoretical background

Wave velocities (V_P and V_S) and electrical resistivity (ρ) in soils depend to a varying degree on porosity, saturation, fabric, stress, mineralogy, pore fluid and temperature (Mavko *et al.*, 1998; Santamarina *et al.*, 2001; Mitchell & Soga, 2005). An electro-seismic model is a system of equations that links some hydrological and mechanical parameters of soil to geophysical parameters. For example, Carrara *et al.* (1994) proposed a model based on the scheme of a rock mass as a polycomponent medium made up of matrix, clay, water and air. Their model was based on the time-average model proposed by Wyllie *et al.* (1956) for seismic velocity and the model of parallel resistors proposed by Patnode & Wyllie (1950) for electrical resistivity.

The model proposed in this paper utilises Archie's law to describe the electrical behaviour of soils and the recent formulation of wave propagation in unsaturated soils proposed by Conte *et al.* (2009). The Archie's law, which holds for porous media with non-conductive solid grains (e.g. clean sands), can be written as

$$\sigma = \sigma_w \phi^p S_r^q \tag{1}$$

where σ and σ_w are respectively the soil and interstitial fluid electrical conductivities, ϕ is the porosity, S_r is the degree of saturation, and p and q are two parameters that take into account the geometry of the interconnected porosity.

The formulation of wave propagation, developed by Conte *et al.* (2009), is based on the theory of linear poro-elasticity in conjunction with the constitutive relationships originally proposed by Fredlund & Morgenstern (1976) to describe the volume changes of unsaturated soils caused by changes in total stress and suction. The theory predicts the existence of three compressional waves and one shear wave in unsaturated porous media. The waves are dispersive, that is, their speed of propagation is frequency dependent (Coussy, 2004). The fastest compressional wave is considered in the following as it is the one that is measured in laboratory and field experiments. The expressions of V_P and V_S are obtained by applying the formulation of Conte *et al.* (2009) to the case of low-frequency excitations

$$V_P^2 = \frac{\dfrac{2(1-\nu^{sk})}{1-2\nu^{sk}} G + \dfrac{\left\{ \begin{array}{l} K^a K^w \left[m_2^w - \dfrac{3(1-2\nu^{sk}) S_r^2}{2(1+\nu^{sk})G} \right] \\ + \phi S_r (1-S_r)[K^w S_r + K^a (1-S_r)] \end{array} \right\}}{\left\{ \begin{array}{l} \phi [K^a S_r + K^w (1-S_r)] \\ \times \left[m_2^w - \dfrac{3(1-2\nu^{sk}) S_r^2}{2(1+\nu^{sk})G} \right] \\ + \phi^2 S_r (1-S_r) \end{array} \right\}}}{(1-\phi)\rho_s + S_r \phi \rho_w + (1-S_r)\phi \rho_a} \tag{2}$$

$$V_S^2 = \frac{G}{(1-\phi)\rho_s + S_r \phi \rho_w + (1-S_r)\phi \rho_a} \tag{3}$$

where G is the shear modulus; υ^{sk} is the Poisson's ratio of the soil skeleton; m_2^w denotes the coefficient of water volume change with respect to a change in matric suction; K^w and K^a are the bulk moduli of water and air respectively; ρ_s, ρ_w and ρ_a are the densities of the solid phase, water phase and air phase respectively. The low frequency assumption is justified by the relatively low operational frequency of seismic sources used for geophysical tests.

The coefficient of volume change for the water phase (m_2^w) can be obtained experimentally from the water retention curve. The water volume content can be described analytically by van Genuchten's equation (van Genuchten, 1980)

$$\theta = \phi S_r = \frac{(\theta_{sat} - \theta_r)}{[1 + (\alpha\psi)^n]^m} + \theta_r \tag{4}$$

where θ_r and θ_{sat} are residual and saturated values of the volumetric water content θ; ψ is the matric suction; α, n and m are experimental parameters.

The coefficient m_2^w can be evaluated by deriving equation (4)

$$m_2^w = \frac{\partial\theta}{\partial\psi} = (\theta_{sat} - \theta_r) \frac{-n \cdot m \cdot \alpha (\alpha\psi)^{n-1}}{[1 + (\alpha\psi)^n]^{m+1}} \tag{5}$$

Combining equation (4) and equation (5), it is possible to write

$$m_2^w = -(\theta - \theta_r) nm\alpha \left(\frac{\theta - \theta_r}{\theta_{sat} - \theta_r} \right)^{1/m} \left[\frac{1}{\left(\dfrac{\theta - \theta_r}{\theta_{sat} - \theta_r} \right)^{1/m}} - 1 \right]^m \tag{6}$$

Formulas for porosity and degree of saturation

The system of equations (1)–(3) and (6) allows the porosity and the degree of saturation to be evaluated from measured wave velocities (V_P, V_S) and electrical conductivity (σ). Indeed, in the previous equations ρ_s, ρ_w, ρ_a, K^w, K^a can be considered as physical parameters with standard values; while the coefficients of Archie's law and van Genuchten's equation can be evaluated through laboratory tests. The Archie's law parameters can be inferred with a simple measurement of electrical conductivity at different porosities and water contents. The parameters of van Genuchten's law can be estimated by fitting data of the water retention curve obtained with well-documented techniques (e.g. pressure plate extractor, suction controlled oedometer cell, filter paper method) (Fredlund & Rahardjo, 1993; Murray & Sivakumar, 2010). Recently Cosentini *et al.* (2012) used electrical tomographic reconstructions in the laboratory to infer van Genuchten's parameters.

Substitution of equations (1), (3) and (6) in equation (2) yields

$$V_P^2 = \frac{2\alpha_{sk} G + [(K^a K^w B + D)/(L B + C)]}{R} \tag{7}$$

where

$$R = (1-\phi)\rho_s + \Gamma \phi^{Q+1} \rho_w + \phi(1 - \Gamma\phi^Q)\rho_a$$

$$L = \phi \left[K^a \Gamma \phi^Q + K^w (1 - \Gamma\phi^Q) \right]$$

$$B = -M(\Gamma\phi^{Q+1} - \theta_r)^{[(1/m)+1]} \lambda \left[(\Gamma\phi^{Q+1} - \theta_r)^{-1/m} \lambda^{-1} - 1 \right]^m - \frac{3\beta_{sk}}{G} \Gamma^2 \phi^{2Q}$$

$$C = \Gamma\phi^{Q+2}(1 - \Gamma\phi^Q)$$

$$D = \Gamma\phi^{Q+1}(1 - \Gamma\phi^{Q})\left[K^{w}\Gamma\phi^{Q} + K^{a}(1 - \Gamma\phi^{Q})\right]$$

$$\Gamma = \left(\frac{\sigma}{\sigma_{w}}\right)^{1/q}$$

$$Q = -\frac{p}{q}$$

$$\alpha_{sk} = \frac{1 - \nu^{sk}}{1 - 2\nu^{sk}}$$

$$\beta_{sk} = \frac{1 - 2\nu^{sk}}{2(1 + \nu^{sk})}$$

$$M = \alpha\, m\, n$$

$$\lambda = \frac{1}{(\theta_{sat} - \theta_{r})^{1/m}}$$

Equation (7) is a non-linear function of porosity. Therefore, the porosity has to be evaluated numerically by solving an inverse problem with an iterative procedure. The objective function to be minimised expresses the discrepancy between the observed and predicted system responses. In this specific case, it is a measure of the difference between the predicted and the measured compressional wave velocities. The L1 norm of the misfit has been chosen as the objective function to limit the weight of outliers (Menke, 1989)

$$\min||e_1|| = \left|\left|V_{P}^{2} - V_{P\,obs}^{2}\right|\right| \tag{8}$$

where V_P and $V_{P\,obs}$ are the calculated and measured values, respectively.

The porosity obtained by equation (8) can be used to evaluate the degree of saturation by

$$S_r = \Gamma\phi^{Q} \tag{9}$$

The shear modulus (G), which is needed to solve the inverse problem of equation (8), depends on the stiffness of the granular skeleton. At constant effective confinement, the stiffness of the soil skeleton varies with the degree of saturation. In general, an increase of the stiffness is observed with decreasing saturation due to contact-level capillary forces, which leads to the development of suction in the pore water.

To take into account the influence of suction on the shear modulus (G), an appropriate relationship is needed to evaluate equation (7).

Many authors have proposed relationships to account for the influence of suction on shear modulus: Wu *et al.* (1984), Qian *et al.* (1993), Marinho *et al.* (1995), Mancuso *et al.* (2002), Fratta *et al.* (2005), Kawajiri *et al.* (2011), Oh & Vanapalli (2011).

For example, neglecting anisotropy effects, for normally consolidated materials a power equation can be used (Mancuso *et al.*, 2002)

$$G = A\, f(e)\left[\frac{(p - u_a) + \psi}{p_r}\right]^{b} \tag{10}$$

where A is a stiffness index, p is the mean total stress, u_a is the air pressure, ψ is the suction, p_r is a reference pressure, b is a fitting parameter and $f(e)$ is a function of void ratio e. Several expressions are available for the void ratio function $f(e)$ as reported in Mitchell & Soga (2005).

Equation (7) can be used to plot a diagram where each curve describes how the electrical conductivity (σ) and the P-wave velocity (V_P) change when porosity is fixed and the degree of saturation is increased, or vice versa. Fig. 1 reports an example for sand. The set of parameters used to draw this diagram is reported in Table 1 with related references. Table 2 presents the assumed standard values of physical parameters: ρ_s, ρ_w, ρ_a, K^w, K^a. In the diagram the range of porosity is limited to 0·2–0·8, typical values for soils, whereas the degree of saturation is assumed to vary between 0·01 and 1·00.

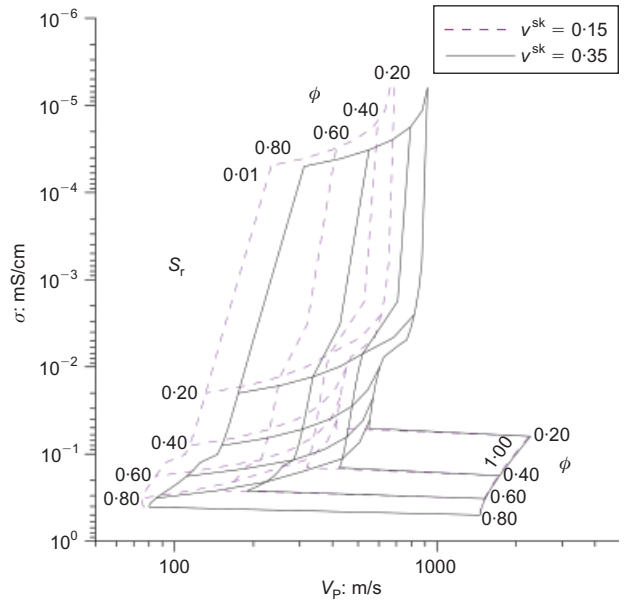


Fig. 1. Examples of velocity–conductivity diagram as a function of porosity and degree of saturation for two values of Poisson ratio of the soil skeleton

Table 2. Assumed values of the physical constants for determining porosity and degree of saturation

ρ_s: kN·s^2/m^4	2·767
ρ_w: kN·s^2/m^4	1·000
ρ_a: kN·s^2/m^4	0·001
K^a: kPa	$1{\cdot}45 \times 10^2$
K^w: kPa	$2{\cdot}25 \times 10^6$
υ^{sk}	0·15 ÷ 0·35

Table 1. Parameters of Archie's law, van Genuchten's equation and equation (10) used to plot the velocity–conductivity diagram in Fig. 1

van Genuchten*		Archie†		Equation (10)‡	
α: kPa^{-1}	0·350	σ_w: mS/cm	0·7	A	140 000
n	3·190	p	1·5	$f(e)$	$1/(0{\cdot}3 + 0{\cdot}7e^2)$
m	0·687	q	2·0	b	0·5
θ_{sat}	0·370			p_r: kPa	100
θ_r	0·058				

* After Tuller & Or (2004).
† After Mitchell & Soga (2005).
‡ After Hardin & Blandford (1989).

A conductivity–velocity diagram, as the one reported in Fig. 1, can be used for a preliminary evaluation of the porosity and the degree of saturation on the basis of measured conductivity and P-wave velocity values.

The effect of the Poisson ratio of the soil skeleton on the evaluation of porosity and degree of saturation is shown in Fig. 1, where two velocity–conductivity diagrams for $v^{sk} = 0{\cdot}15$ (dashed lines) and $v^{sk} = 0{\cdot}35$ (continuous lines) are plotted. In particular, in the range of degree of saturation between 0·9 and 1, it is possible to observe a flat zone in which the influence of Poisson ratio can be neglected. In general, Poisson ratio has significant control on the evaluation of porosity and less influence on the degree of saturation. In any case, the differences are limited and comparable with usual experimental uncertainties.

Shear modulus–suction relationship

The proposed procedure requires variations of the shear modulus (G) with respect to suction to be taken into account.

Many experimental investigations have been performed on coarse- and fine-grained soils to investigate the effect of suction stress on the shear stiffness of soils (Wu *et al.*, 1984; Qian *et al.*, 1991, 1993. Marinho *et al.*, 1995; Cho & Santamarina, 2001; Mancuso *et al.*, 2002; Kawajiri *et al.*, 2011; Oh & Vanapalli, 2011). Two typical trends have been individuated (Oh & Vanapalli, 2011): shear modulus monotonically increasing with increasing suction (typical of fine-grained soils) or shear modulus reaching a peak at an intermediate saturation state and then decreasing for increasing suction (observed in many experiments on coarse-grained soils). Cho & Santamarina (2001) provided possible explanations for this observed difference.

A new relationship which describes the influence of suction on shear modulus is proposed below

$$G(S) = G_{sat}\left\{1 + \left[\frac{\psi_{res} - \psi_{aev}}{2p_r}\left(-\frac{\partial\theta}{\partial\psi}\psi\right)\left(\frac{n}{2}\right)\left(\frac{m}{1-m}\right)\right] \times (1 - S_r)^{(m/1+m)}\right\} \tag{11}$$

where G_{sat} is the shear modulus under saturated condition, ψ_{res} is the residual suction value, ψ_{aev} is the air entry value, p_r is a reference pressure, and n and m are the parameters of van Genuchten's equation. This expression reproduces the stiffness variation with the degree of saturation with a continuous function and without introducing additional parameters.

The relation given by equation (11) takes into account that the evolution of suction depends on the variation of degree of saturation; therefore, the effects of suction on shear stiffness have to be associated with the soil water retention curve.

Equation (11) has been validated using the experiments by Wu *et al.* (1984) on Glacier Way silt (particle size distribution between 0·0001 and 0·2 mm with a uniformity coefficient $C_U = 125$). The parameters n, m, ψ_{sat} and ψ_{aev} were evaluated fitting the water retention curve by Wu *et al.* (1984) with van Genuchten's equation (Fig. 2). The experimental points of the water retention curve (Fig. 2) were obtained by pressure plate extractor. Fig. 3 shows that equation (11) closely follows the variation of shear modulus plotted against degree of saturation that Wu *et al.* (1984) observed in their resonant column tests.

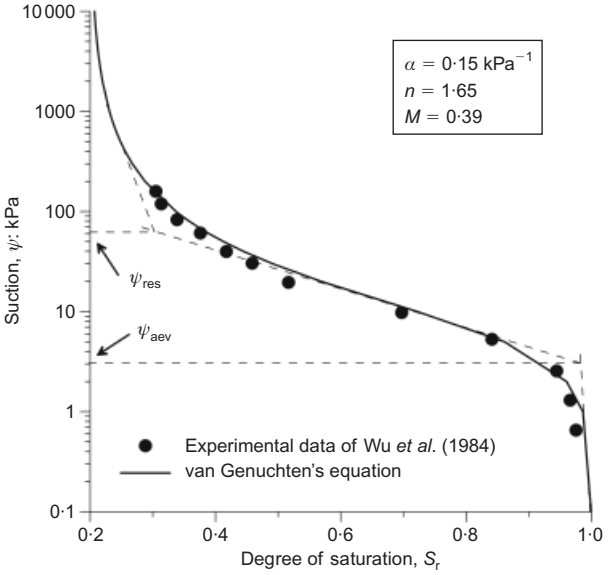


Fig. 2. Observed and calculated water retention curve for experimental data by Wu *et al.* (1984) (range of the particle diameter is from 0·0001 to 0·2 mm)

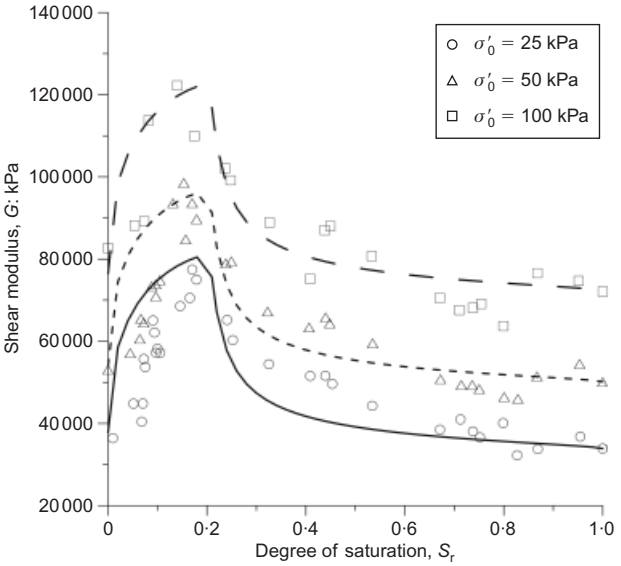


Fig. 3. Shear modulus plotted against degree of saturation: comparison between experimental data by Wu *et al.* (1984) and the proposed relationship (equation (11))

LABORATORY EXPERIMENTAL DATA

Laboratory data are used to verify the proposed approach. The data are taken from the work of Comina *et al.* (2010). Main features of the experiments are described below. The experiments were conducted on uniform quartz sand samples (range of particle diameter was from 0·08 to 0·4 mm, uniformity coefficient $C_U = 2{\cdot}7$ and specific gravity of solids $G_s = 2{\cdot}767$).

Water retention curve

The water retention curve was obtained by measuring matric suction using the filter paper method (ASTM D 5298-94 (ASTM, 1997)) on duplicate samples prepared by compacting a mixture of soil and preselected quantities of distilled water with the moist tamping technique at a porosity $\phi = 0{\cdot}4$. Whatman No. 2 filter papers were placed in direct contact with the samples, as prescribed by the standard

procedure. Each specimen with filter paper was then placed in an airtight container and left in a temperature-controlled room (20 ± 1°C) for 7 d. The ASTM (1997) filter paper calibration curve (ASTM D 5298-94) was used. Experimental data and van Genuchten's fitting equation are shown in Fig. 4, while the fitting parameters are reported in Table 4.

Seismic and electrical measurements

Seismic and electrical measurements were performed in a special oedometer cell, designed to perform geophysical tests (Comina *et al.*, 2008). The cell is equipped for three-dimensional (3D) electrical resistivity tomography (ERT) and to measure the velocity of compression (P) and shear (S) seismic waves. The cell has 42 electrodes located on its internal boundary: 16 are equally spaced on the sidewall, and 13 are on each base and top plates. On each plate, there are a bender element and an extender plate for the measurement of S- and P-wave velocities, respectively.

The samples were prepared by mixing soil and 0·1 M potassium chloride in water solution at given degrees of saturation in the range between 20 and 100%. Salt solution was used as the liquid phase to ensure a constant value of interstitial fluid electrical conductivities (σ_w) during electrical resistivity measurements. To obtain samples with height of 4 cm and homogeneous density, the soil was compacted in four layers at an average porosity $\phi = 0{\cdot}4$ directly in the oedometer cell using the moist tamping technique.

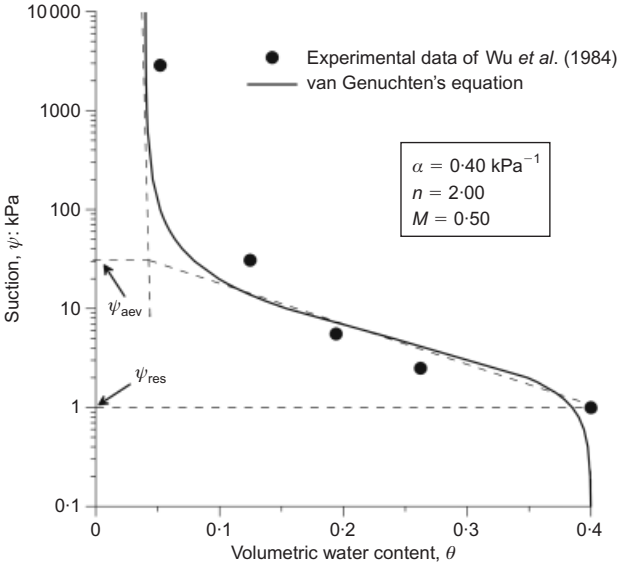


Fig. 4. Observed and calculated water retention curve for the investigated soil (range of the particle diameter is from 0·08 to 0·4 mm).

Electrical conductivity. The ERT was performed on each sample. About 800 electrical resistivity measurements were performed for each tomography. The measurement protocol combines 'horizontal' measurements, in which the pairs of electrodes that apply electrical current and those that measure electrical potential are on the sidewall; 'vertical' measurements, in which both couples of electrodes are on the base and top plates; and 'mixed' measurements, in which the electrodes that apply electrical current are on the sidewall and the measuring electrodes are on the plates. This sequence allows a good reconstruction of the distribution of the electrical conductivity within the sample. Details on least-squares inversion algorithm can be found in Borsic *et al.* (2005).

The tomographic reconstructions showed an almost homogeneous distribution of conductivity for each sample, so the average conductivity was considered in the present work (Table 3). The electrical conductivity plotted against degree of saturation relationship is shown in Fig. 5 in non-dimensional form (σ/σ_w). Since the soil is a quartz sand, the assumption of 'non-conductive particle model' (Mitchell & Soga, 2005) is justified, and Archie's law can be appropriately applied to fit these experimental data. The p and q exponents of the Archie's law are reported in Table 4.

Table 3. Values of conductivity (σ) and P- and S-wave velocities measured in laboratory tests. Values of shear modulus G estimated with equation (3) are also reported

	S_r	V_P: m/s	V_S: m/s	G:* kPa	σ: mS/cm
$\phi = 0{\cdot}4$	0·20	293	197	67 256	0·1677
	0·34	339	232	95 956	0·3163
	0·41	335	212	81 422	0·4729
	0·59	376	194	71 115	0·7671
	0·61	350	201	76 462	0·7684
	0·72	348	194	72 946	0·9762
	0·82	283	173	59 538	1·2000
	0·92	261	172	59 760	1·4000
	0·99	1259	127	33 182	1·6000

* Evaluated from S-wave velocity measurements with equation (3).

Table 4. Fitting parameters of Archie's law, van Genuchten and equation (11) for the laboratory specimens

van Genuchten		Archie		Equation (11)	
α: kPa^{-1}	0·40	σ_w: mS/cm	13·98	ψ_{res}: kPa	30
n	2·00	p	2·29	ψ_{aev}: kPa	1
m	0·50	q	1·64	G_{sat}: kPa	33 182
θ_{sat}	0·40				
θ_r	0·04				

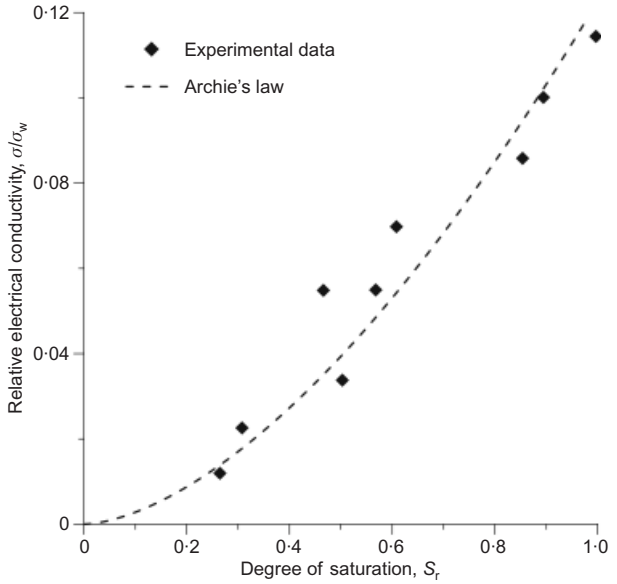


Fig. 5. Relationship between electrical conductivity and degree of saturation at constant void ratio for the laboratory test

Seismic wave velocities. Wave velocity measurements of each sample were performed using bender elements and extender plates to generate and receive the S- and P-wave respectively; a function generator to excite the transducers with a single sinusoidal signal; and an oscilloscope to record the traces. The extender and bender transducers were excited with sinusoidal signal of 50 kHz and 10 kHz apparent frequency, respectively. The travel time of each wave was detected on recorded trace operating a first arrival picking. The choice of frequency was operated to assure a good quality of traces and to prevent the near-field effect for the S-wave.

P- and S-waves velocities of the specimen for each degree of saturation (S_r) are reported in Table 3. Figure 6 shows wave velocities (V_P and V_S) measured at different values of the degree of saturation. The trends are similar to those published by previous authors (e.g. Wu *et al.*, 1984; Qian *et al.*, 1991, 1993).

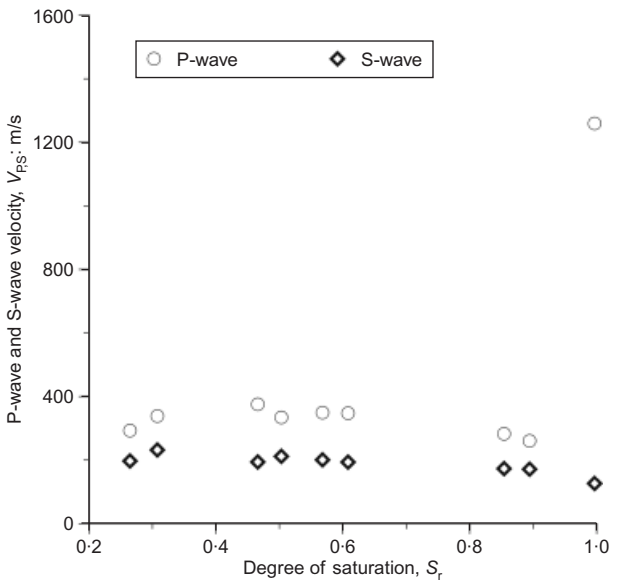


Fig. 6. Seismic wave velocities measured at different degrees of saturation in the laboratory

APPLICATION OF THE PROCEDURE AND DISCUSSION OF THE RESULTS

The proposed procedure is here applied to the dataset described in the previous section.

For one, equation (11) was used to describe the variation of shear modulus (Table 3) evaluated by S-wave velocity measurements plotted against the degree of saturation for the dataset of the present paper (Fig. 7). The obtained parameters are reported in Table 4.

Figure 7 shows that equation (11) is able to describe the trend of experimental data in spite of the small local differences between the experimental data and predicted values. Some differences can also be observed in Fig. 3 for the experimental data of Wu *et al.* (1984), especially at saturation levels lower than 0·5 and for pressure of 25 kPa. Experimental uncertainties are likely to be the cause of these local differences. In both applications of equation (11) (Figs 3 and 7), it is possible to observe how the water retention curve influences the prediction of shear moduli. The shape of the retention curve depends on material properties including pore size distribution, grain size distribution, density, organic material content, clay content and mineralogy (Lu & Likos, 2004). In general, poorly graded soils (e.g. uniform sand) tend to drain more easily than well-graded soils (e.g. silt, clay). Hence the first type of soils is marked by relatively flat water retention curves in the capillary regime because the majority of pores are drained over a relatively narrow range of suction (Lu & Likos, 2004). The shape of water retention curve in the capillary regime zone strongly influences the term in the square parenthesis in equation (11). For example, in poorly graded soils the evoked term of equation (11) is less affected by the change of suction. These aspects may explain the reason for the different sensitivity of equation (11) in the prediction of shear moduli for silty and sandy soils.

Finally, equation (7) and equation (11) were used to construct a velocity–conductivity diagram for the present dataset. The required model parameters are reported in Table 4 and Table 2. Fig. 8 shows the P-wave velocities and average values of conductivity measured in the laboratory in a velocity–conductivity diagram. The experimental data are located close to the 0·4 porosity line in the range 0·2–1·00 for the degree of saturation, which are the values of ϕ and S_r imposed in the tests.

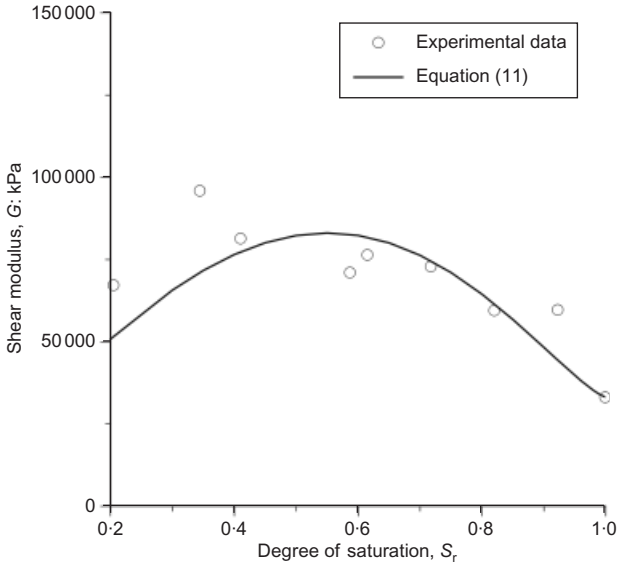


Fig. 7. Shear modulus plotted against degree of saturation for the laboratory test: comparison between experimental data and the proposed relationship (equation (11))

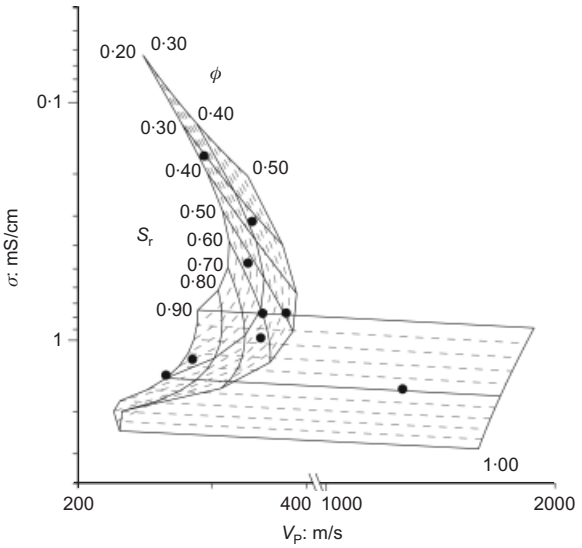


Fig. 8. Velocity–conductivity diagram with laboratory experimental data

In Figs 9(a) and 9(b) the values of porosity and degree of saturation imposed in the experimental tests are compared to the values inferred with the proposed approach on the basis of geophysical measurements. The figures show that the average error in the evaluation of porosity is 10%, whereas the error is higher for the evaluation of the degree of saturation.

The difference between calculated and imposed porosity plotted against measured degree of saturation is shown in Fig. 10(a), while the difference for the degree of saturation is plotted in Fig. 10(b). Larger discrepancies are observed for degree of saturation lower than 0·80.

The principal causes of the disagreement may be associated with

(*a*) errors in the evaluation of seismic velocities
(*b*) errors in the measurements of average conductivity
(*c*) choice of soil skeleton Poisson ratio
(*d*) errors in the evaluation of the water retention curve.

The first three causes appear to be negligible for the following reasons.

(*a*) For P-wave velocity measurements, first arrival picking was operated on traces recorded with an oscilloscope with a sampling time of 1 μs. The height of each sample was measured with a tolerance of 0·5 mm. Therefore, the maximum errors in P-wave velocity measurements can generate maximum errors of 2% on the degree of saturation and of 0·5 % on the porosity, which are much less than those observed in Figs 9(a), 9(b) and 10. Moreover, these errors can be considered independent of the saturation, otherwise the trend of Fig. 10 would not have been observed. Analogous considerations apply for S-waves velocity measurements.
(*b*) The average electrical conductivity was calculated with a largely redundant number of electrical resistivity measurements acquired for ERT, hence it is possible to consider this measurement very accurate. Furthermore, maximum errors in electrical conductivity should be recorded at low saturation, but Fig. 10 shows that the maximum errors in the evaluation of unknowns (ϕ and S_r) are not at low saturation.
(*c*) Figure 1 shows that the assumption on the soil skeleton Poisson ratio affects the porosity independently from the degree of saturation, hence a wrong assumption on Poisson ratio cannot explain the larger discrepancies for intermediate saturation degree observed in Fig. 10.

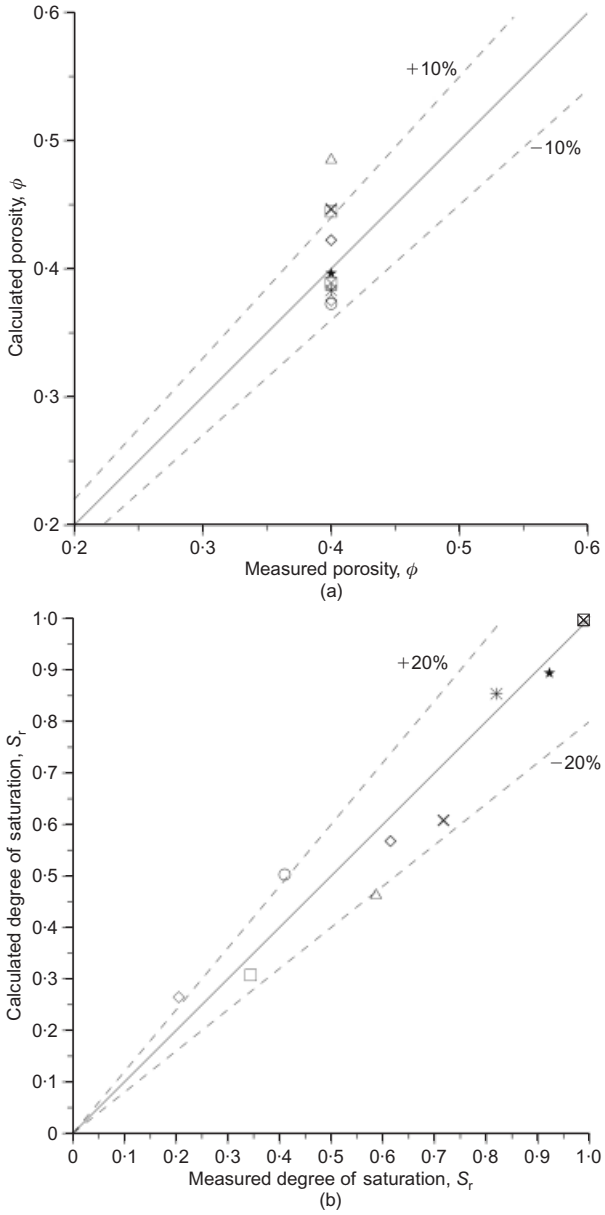


Fig. 9. Comparison between experimental and calculated (a) porosity and (b) degree of saturation of laboratory specimens

Eventually, errors in the water retention curve may be considered the most plausible cause of discrepancies in Fig. 10. Indeed, suction measurements are not easy; they are very time consuming and sensitive to testing technique. In the present tests, the measurements of suction were performed using the filter paper method. This technique estimates the suction of soil indirectly by simple measurements of the moisture content of a filter paper at the same suction as the soil. Although this method is very simple, careful procedures must be used to avoid erroneous measurements (e.g. a room with constant temperature and a sufficient equilibration time are required) (Bulut & Leong, 2008). The suction of soil is obtained from the calibration curve of the filter paper water content with suction. Supposing a careful setting of the method, the evaluation of moisture content of filter paper is the principal cause of errors in the suction measurements. The major errors can be committed when measuring small masses of the filter paper moisture, because on the basis of the calibration curve, small differences of filter paper moisture correspond to large values of suction.

Another source of error can be associated with the difference between the experimental data of the water reten-

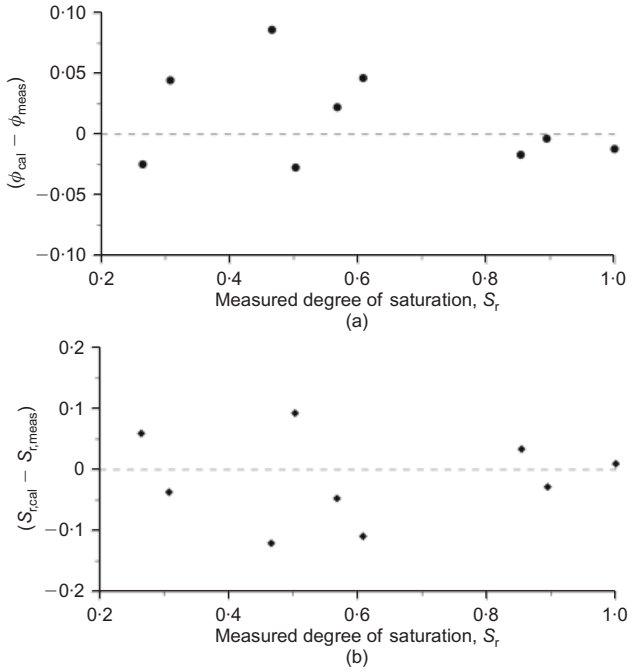


Fig. 10. Errors in the evaluation of (a) porosity and (b) degree of saturation plotted against measured degree of saturation of laboratory specimens

tion curve and the values predicted by the van Genuchten's expression. Indeed the latter is used in the seismo-electric model and these discrepancies at intermediate degrees of saturation may justify the observed trends of Fig. 10. From this point of view, other analytical expressions of the water retention curve may provide an improvement on the seismo-electric model.

Although some differences between experimental data and the model can be observed, such discrepancies can be considered acceptable from an engineering viewpoint. Indeed, the method allows the evaluation of the porosity and degree of saturation for coarse-grained soils, where it is complicated to obtain undisturbed samples and where the traditionally adopted methods (e.g. empirical correlations with penetration tests) are affected by large uncertainties.

CONCLUSIONS

A procedure has been presented for an evaluation of porosity and degree of saturation of unsaturated soils from electrical conductivity and seismic wave velocities measurements. The proposed procedure is relevant in geotechnical engineering practice, considering that it may be very useful when undisturbed sampling is not feasible.

It requires measurements of electrical conductivity and P- and S-wave velocities. These quantities can be obtained by geophysical tests, which allow soils to be investigated in their natural state on site. Other parameters required for the calibration of the electro-seismic model may be obtained in the laboratory on disturbed samples, or alternatively through the use of empirical relationships or, better, with additional information, as for example measurements of suction (e.g. tensiometer) or moisture content (e.g. capacitance/frequency-domain reflectometry probes (FDR), time-domain reflectometry probes (TDR), dual needle heat pulse probes).

Because for the proposed procedure, a relationship of shear modulus against degree of saturation was needed, a new relationship has been proposed in the form of a continuous function based on the van Genuchten's parameters of the water retention curve. The formula has been validated according to the literature data and then used to fit the available experimental data for the present study.

Geophysical measurements performed in the laboratory on uniform sand samples compacted at an average porosity ($\phi = 0{\cdot}4$) and at different initial mass water contents have been used to validate the proposed electro-seismic model.

Results from this preliminary investigation show that the average error in the evaluation of porosity is 10%, whereas the error is higher for the evaluation of the degree of saturation. The possible causes of errors have been analysed and discussed, concluding that the major source of uncertainty is likely to be associated with the measurement and representation of the water retention curve.

Although a more extensive experimental programme is required for full validation of the model, the preliminary results obtained on the available dataset are encouraging. The method is principally devised to investigate intermediate and coarse-grained soils, therefore the observed accuracy is acceptable if compared to other available approaches. The proposed procedure can be considered promising for the characterisation and monitoring of unsaturated soil deposits on the basis of field geophysical tests.

NOTATION

A	stiffness index
b	fitting parameter of equation (10)
e	void ratio
$f(e)$	function of void ratio
G	shear modulus
G_{sat}	shear modulus under saturated condition
K^a	bulk modulus of air
K^w	bulk modulus of water
m	parameter of van Genuchten's equation
m_2^w	coefficient of water volume change with respect to a change in matric suction
$\min\|\|e_1\|\|$	minimum of L1 norm of the misfit
n	parameter of van Genuchten's equation
p	parameter of Archie's law
$p - u_a$	net total stress
p_r	reference pressure
q	parameter of Archie's law
S_r	degree of saturation
V_P	seismic P-wave velocity
$V_{P\,obs}$	measured value of seismic P-wave velocity
V_S	seismic S-wave velocity
α	parameter of van Genuchten's equation
$\frac{\partial\theta}{\partial\psi}$	derivative of volumetric water content with regard to the matric suction
θ	volumetric water content
θ_r	residual value of the volumetric water content
θ_{sat}	saturated value of the volumetric water content
υ^{sk}	Poisson ratio of the soil skeleton
ρ	electrical resistivity
ρ_a	density of air phase
ρ_s	density of solid phase
ρ_w	density of water phase
σ	soil electrical conductivity
σ_w	interstitial fluid electrical conductivity
σ'_0	effective confining pressure
ϕ	soil porosity
ψ	matric suction
ψ_{aev}	air entry value
ψ_{res}	residual suction value

REFERENCES

Archie, G. E. (1942). The electrical resistivity log as an aid to determining some reservoir characteristics. *Trans. Am. Inst. Mining, Metallurgical and Petroleum Engrs* **146**, 54–62.

ASTM (1997). D 5298-94: Standard test method for measurement

of soil potential (suction) using filter paper. West Conshohocken, PA, USA: ASTM International.

Biot, M. A. (1956a). Theory of propagation of elastic waves in a fluid-saturated porous solid. I. Low-frequency range. *J. Acoust. Soc. Am*. **28**, No. 2, 168–178.

Biot, M. A. (1956b). Theory of propagation of elastic waves in a fluid-saturated porous solid. II. Higher-frequency range. *J. Acoust. Soc. Am*. **28**, No. 2, 179–191.

Borsic, A., Comina, C., Lancellotta, R., Foti, S. & Musso, G. (2005). Imaging heterogeneities in sand samples with electrical impedance tomography: laboratory results. *Géotechnique* **55**, No. 7, 539–547, http://dx.doi.org/10.1680/geot.2005.55.7.539.

Bulut, R. & Leong, E. C. (2008). Indirect measurement of suction. *Geotech. Geol. Engng* **26**, No. 6, 633–644.

Carrara, E., Pece, R. & Roberti, N. (1994). Geoelectrical and seismic prospection in hydrogeology: model and master curves for the evaluation of porosity and water saturation. *Pure Appl. Geophys*. **143**, No. 4, 729–751.

Cho, G. C. & Santamarina, J. C. (2001). Unsaturated particulate materials – particle level studies. *J. Geotech. Geoenviron. Engng* **127**, No. 1, 84–96.

Comina, C., Foti, S., Sambuelli, L., Socco, L. V. & Strobbia, C. (2002). Joint inversion of VES and surface wave data. *Proceedings of SAGEEP 2002*, Las Vegas, USA (CD-ROM). Denver, CO, USA: Environmental and Engineering Geophysical Society.

Comina, C., Foti, S., Musso, G. & Romero, E. (2008). EIT oedometer – an advanced cell to monitor spatial and time variability in soil. *Geotech. Test. J. ASTM* **31**, No. 5, 404–412.

Comina, C., Cosentini, R. M., Foti, S. & Musso, G. (2010). Electrical tomography as laboratory monitoring tool. *Riv. Ital. Geotec.* **44**, No. 1, 15–26.

Conte, E., Cosentini, R. M. & Troncone, A. (2009). Shear and dilatational wave velocities for unsaturated soils. *Soil Dynam. Earthquake Engng* **29**, No. 9, 946–952.

Cosentini, R. M., Della Vecchia, G., Foti, S. & Musso, G. (2012). Estimation of the hydraulic parameters of unsaturated samples by electrical resistivity tomography. *Géotechnique* **62**, No. 7, 583–594, http://dx.doi.org/10.1680/geot.10.P.066.

Coussy, O. (2004). *Poromechanics*. Chichester, UK: Wiley.

Foti, S. & Lancellotta, R. (2004). Soil porosity from seismic velocities. *Géotechnique* **54**, No. 8, 551–554, http://dx.doi.org/10.1680/geot.2004.54.8.551.

Foti, S., Lai, C. G. & Lancellotta, R. (2002). Porosity of fluid-saturated porous media from measured seismic wave velocities. *Géotechnique* **52**, No. 5, 359–373, http://dx.doi.org/10.1680/geot.2002.52.5.359.

Foti, S., Sambuelli, L., Socco, L. V. & Strobbia, C. (2003). Experiments of joint acquisition of seismic refraction and surface wave data. *Near Surface Geophys. EAGE* **1**, No. 3, 119–129.

Fratta, D., Alshibli, K. A., Tanner, W. M. & Roussel, L. (2005). Combined TDR and P-wave velocity measurements for the determination of in situ soil density – Experimental study. *Geotech. Test. J. ASTM* **28**, No. 6, 553–563.

Fredlund, D. G. & Morgenstern, N. R. (1976). Constitutive relations for volume change in unsaturated soils. *Can. Geotech. J.* **13**, No. 3, 261–276.

Fredlund, D. G. & Rahardjo, H. (1993). *Soil mechanics for unsaturated soils*. New York, NY, USA: John Wiley.

Hardin, B. O. & Blandford, G. E. (1989). Elasticity of particulate materials. *J. Geotech. Engng, ASCE* **115**, No. 6, 788–805.

Hofman, B. A., Sego, D. C. & Robertson, P. K. (2000). In situ ground freezing to obtain undisturbed samples of loose sand. *J. Geotech. Geoenviron. Engng* **126**, No. 11, 979–989.

Kawajiri, S., Shibuya, S., Kato, S. & Kawaguchi, T. (2011). Effects of matric suction on elastic shear modulus for three unsaturated soils. In *Unsaturated soils, proceedings of the 5th international conference on unsaturated soils* (eds E. Alonso and A. Gens), pp. 271–275. London, UK: Taylor & Francis Group.

Lancellotta, R. (2009). *Geotechnical engineering*. London, UK: Taylor and Francis.

Lu, N. & Likos, W. J. (2004). *Unsaturated soil mechanics*. Hoboken, NJ, USA: Wiley.

Mancuso, C., Vassallo, R. & d'Onofrio, A. (2002). Small strain behavior of a silty sand in controlled-suction resonant column – torsional shear tests. *Can. Geotech. J.* **39**, No. 1, 22–31.

Marinho, F. A. M., Chandler, R. J. & Crilly, M. S. (1995). Stiffness measurements on an unsaturated high plasticity clay using bender elements. In *Unsaturated soils, proceedings of the 1st international conference on unsaturated soils* (eds E. Alonso and P. Delage), pp. 535–539. Rotterdam, the Netherlands: A. A. Balkema.

Mavko, G. M., Mukerji, T. & Dvorkin, J. (1998). *The rock physics handbook*. New York, NY, USA: Cambridge University Press.

Menke, W. (1989). *Geophysical data analysis: discrete inverse theory.* San Diego, CA, USA: Academic Press.

Mitchell, J. K. & Soga, K. (2005). *Fundamentals of soil behavior*. New York, NY, USA: John Wiley.

Murray, E. J. & Sivakumar, V. (2010). *Unsaturated soils: a fundamental interpretation of soil behaviour*. Chichester, UK: Wiley-Blackwell.

Oh, W. T. & Vanapalli, S. K. (2011). The relationship between the elastic and shear modulus of unsaturated soils. In *Unsaturated soils, proceedings of the 5th international conference on unsaturated soils* (eds E. Alonso and A. Gens), pp. 341–346. London, UK: Taylor & Francis Group.

Patnode, H. W. & Wyllie, M. R. J. (1950). The presence of conductive solids in reservoir rock as a factor in electric log interpretation. *Trans. Am. Inst. Mining, Metallurgical and Petroleum Engrs* **189**, 47–52 (cited in Carrara *et al.* (1994)).

Qian, X., Gray, D. H. & Woods, R. D. (1991). Resonant column tests on partially saturated sands. *Geotech. Testing J.* **14**, No. 3, 266–275.

Qian, X., Gray, D. H. & Woods, R. D. (1993). Void and granulometry: effects and shear modulus of unsaturated soils. *J. Geotech. Engng* **119**, No. 2, 295–314.

Santamarina, J. C., Fam, M. & Klein, K. A. (2001). *Soils and waves: particulate materials behavior, characterization and process*. New York, NY, USA: Wiley.

Tuller, M. & Or, D. (2004). Water retention and characteristic curve. In *Encyclopedia of soils in the environment* (ed. D. Hillel), vol. 4, pp. 278–289. Oxford, UK: Elsevier.

van Genuchten, M. Th. (1980). A closed-form equation for predicting the hydraulic conductivity of unsaturated soils. *Soil Sci. Soc. Am. J.* **44**, No. 5, 892–898.

Wu, S., Gray, D. H. & Richart, F. E. Jr (1984). Capillary effects on dynamic modulus of sands and silts. *J. Geotech. Engng, ASCE* **110**, No. 9, 1188–1203.

Wyllie, M. R. J., Gregory, A. & Gardner, G. H. F. (1956). Elastic wave velocities in heterogeneous and porous media. *Geophys*. **XXI**, No. 1, 41–70 (cited in Carrara *et al.* (1994)).